Journal of Sound and Vibration (1997) **206**(4), 487–505

IDENTIFICATION OF LINEAR TIME-VARYING SYSTEMS

K. Liu

Department of Mechanical Engineering, Faculty of Engineering, Dalhousie University, Halifax, Nova Scotia, B3H 3J5, Canada

(*Received* 3 *July* 1996, *and in final form* 30 *April* 1997)

This paper is concerned with the identification of linear time-varying systems. The discrete-time state space model of freely vibrating systems is used as an identification model. The focus is placed on identifying successive discrete transition matrices that have the same eigenvalues as the original transition matrices. First a typical subspace-based method is presented to illustrate the extraction of the observability range space using the singular value decomposition (SVD) of a general Hankel matrix. Then, the identification of varying transition matrices is approached by using an ensemble of response sequences. For arbitrarily varying systems, a series of the Hankel matrices are formed by an ensemble set of responses which are obtained through multiple experiments on the system with the same time-varying behavior. The varying transition matrix at each moment is estimated through the SVD of two successive Hankel matrices. The proposed algorithm is applied to two special cases that require only a single response series, i.e., periodically varying systems and slowly varying systems. The use of the eigenvalues of the transition matrices is discussed and the pseudomodal parameters are defined. Finally, a two-link manipulator subjected to a varying end force is used as an example to illustrate the tracking capability and performance of the proposed algorithm.

1. INTRODUCTION

Linear time-varying (LTV) systems have been frequently used to model systems that have non-stationary properties and undergo small magnitude vibrations. The identification of LTV systems has received increasing attention. In electrical engineering, many studies on the identification of varying systems have been reported [1]. Early attempts in this direction simply extended the identification techniques of linear time-invariant (LTI) systems to short length outputs of slowly varying (quasi-stationary) systems [2]. Adaptive methods use recursive algorithms to minimize the output error of a parametric system model whose parameters change with time [3]. To improve the tracking ability, the varying parameters of a model are assigned to have a known structure such as a time polynomial or a series of harmonics terms. This way, the problem becomes the estimation of the coefficients of the known structure [4, 5]. In reference [6], the above methods are called the first class approach, namely, the use of a single time sequence of input and output quantities. The second class approach is called ensemble methods which employ multiple input and output sequences, each exhibiting the same underlying time-varying behavior [6–8]. Ensemble methods make it possible to use standard time-invariant system identification techniques because the input and output data are chosen from the same point in the system variation, across an ensemble of responses, rather than over the time course of a single response.

On the other hand, in mechanical engineering, studies of LTV systems have been wide spread. The parametric excitation problems have been investigated by many researchers

0022–460X/97/390487 + 19 $25.00/0/sv971105

[9–12]. The response bound problem of systems with stochastic parameters was addressed in reference [13]. The forced responses of a slowly varying system were investigated in references [14, 15]. A systematic study of LTV mechanical systems was conducted in reference [16]. A time-limited varying pattern was studied in reference [17] and several identification methods of such variation were investigated. However, it is noted that the identification of LTV systems remains a relatively inactive area that deserves more attention.

Modelling a LTV system is another important issue in identification. An ARMA (autoregressive, moving average) model with varying coefficients is a popular choice in using the adaptive estimate methods [3–5]. The varying kernel function or two-dimensional impulse function provides another alternative [18]. Since these models were originally proposed for scalar (single-input and single-output) systems, the use of them is quite cumbersome in the case of multivariable systems. Therefore, the preferred model for more complex problems is a state space model. The popularity of the state space model is also due to the recent development in the subspace-based methods for state space model realization. In the case of LTI systems, the subspace methods can provide accurate state space models for multivariable LTI systems directly from input-output data [19–21].

In the past decade, the subspace methods have been employed to construct so-called time domain state space identification methods in the modal testing community. The Eigensystem Realization Method (ERA) [22] obtained a state space model from Markov parameters. The method used the singular value decomposition (SVD) of the Hankel matrix to extract the observability and controllability matrices. The recursive form of ERA proposed in reference [23] extracted the observability range space using the QR decomposition. The Observability Range Space Extraction (ORSE) identification algorithm [24] was developed by generalizing the Q-Markov Covariance Equivalent Realization (Q-Markov Cover) [25] and the ERA identification algorithms. Comparison of several system identification methods was presented in reference [26]. A SVD-based identification method and the several important uses of the SVD were discussed in reference [27]. However, all the aforementioned studies have been limited to the identification of LTI systems.

Some efforts have been made in extending the subspace-based methods to LTV systems. In reference [7], a solution was presented to identify a state space model from a collection of impulsive responses, each being the response to an input impulse given at consecutive time instances. The work reported in reference [8] extended this solution to the identification of a state space model from an ensemble of input and output data. The study presented in this paper discusses a subspace-based algorithm that uses free responses to identify successive discrete transition matrices of LTV systems. With respect to the previous work, the present paper has two main features: first the focus of the study is placed on finding an identification algorithm that guarantees the invariability of the eigenvalues of the estimated transition matrix. This characteristic differentiates the proposed method from the method proposed in reference [8]. The method in reference [8] results in transition matrices that satisfy the similarity transformation but no longer share the eigenvalues of the original transition matrices. Second, the study is motivated to extend the modal concepts of LTV systems. It proposes the concept of the pseudomodal parameters that are determined from the eigenvalues of the varying transition matrix. The paper explores the use of the pseudomodal parameters to characterize LTV systems.

The paper is organized as follows. Section 2 introduces a SVD-based method for the identification of time-invariant discrete-time state space model using free responses. The first part of section 3 develops an algorithm to identify the discrete transition matrices of arbitrarily time-varying systems using an ensemble of response sequences. The second part

of section 3 extends the proposed algorithm to two special time-varying systems which require only a single response sequence. Section 4 discusses how to use the eigenvalues of the estimated transition matrices to characterize properties of LTV systems. Section 5 presents an example to illustrate the use of the proposed method. Section 6 is a brief conclusion.

2. IDENTIFICATION OF TIME-INVARIANT SYSTEMS

The state space representation of a $p/2$-degree-of-freedom linear time-invariant and freely vibrating system is given by

$$\dot{\mathbf{x}}(t) = \mathbf{A}\mathbf{x}(t), \mathbf{x}(0); \qquad \mathbf{y}(t) = \mathbf{C}\mathbf{x}(t), \tag{1}$$

where $\mathbf{x}(t) \in \mathfrak{R}^p$ is the state variable vector, $\mathbf{x}(0)$ is the initial state, $\mathbf{A} \in \mathfrak{R}^{p \times p}$ is the constant parameter matrix, $\mathbf{C} \in \mathfrak{R}^{n \times p}$ is the constant matrix, and $\mathbf{y}(t) \in \mathfrak{R}^n$ is the response vector. The corresponding discrete-time state space model is of the form

$$\mathbf{x}(k+1) = \mathbf{G}\mathbf{x}(k), \mathbf{x}(0); \qquad \mathbf{y}(k) = \mathbf{C}\mathbf{x}(k), \tag{2}$$

where $\mathbf{G} \in \mathfrak{R}^{p \times p}$ is the state transition matrix given by

$$\mathbf{G} = \exp(\mathbf{A}\Delta t), \tag{3}$$

where Δt is the sampling interval. The solution of equation (2) is

$$\mathbf{y}(k) = \mathbf{C}\mathbf{x}(k) = \mathbf{C}\mathbf{G}^k\mathbf{x}(0). \tag{4}$$

The description of equation (2) is not unique. Let $\mathbf{T} \in \mathfrak{R}^{p \times p}$ be any non-singular matrix and define a new state vector $\mathbf{z} = \mathbf{T}\mathbf{x}$. Replacing $\mathbf{x}$ by $\mathbf{T}^{-1}\mathbf{z}$ in equation (2) results in

$$\mathbf{z}(k+1) = \bar{\mathbf{G}}\mathbf{z}(k), \qquad \mathbf{y}(k) = \bar{\mathbf{C}}\mathbf{z}(k), \tag{5}$$

where $\bar{\mathbf{G}} = \mathbf{T}\mathbf{G}\mathbf{T}^{-1}$ and $\bar{\mathbf{C}} = \mathbf{C}\mathbf{T}^{-1}$ are said to be similarly equivalent to $\mathbf{G}$ and $\mathbf{C}$, respectively. One of the important properties of the similarity transformation is that of $\mathbf{G}$ and $\bar{\mathbf{G}}$ share the same eigenvalues, i.e.,

$$\mathbf{G} = \mathbf{V}\mathbf{\Lambda}\mathbf{V}^{-1} \text{ or } \bar{\mathbf{G}} = (\mathbf{T}\mathbf{V})\mathbf{\Lambda}(\mathbf{T}\mathbf{V})^{-1}, \tag{6}$$

where $\mathbf{V}$ is the eigenvector matrix and $\mathbf{\Lambda}$ is the diagonal eigenvalue matrix, i.e.,

$$\mathbf{\Lambda} = \operatorname{diag}(\lambda_1, \lambda_2, \ldots, \lambda_p). \tag{7}$$

For underdamped mechanical structures, the p eigenvalues and eigenvectors occur in pairs to represent $p/2$ natural modes of vibration. Therefore, the eigenvalues are arranged in such a way that $\lambda_i = \lambda^*_{i+p/2} = \exp(-\delta_i \Delta t + \mathrm{j}\omega_{di}\Delta t)$, where δ_i is the ith damping factor and ω_{di} is the ith damped natural frequency, and $\mathrm{j} = \sqrt{-1}$.

A block Hankel matrix is formed as

$$\mathbf{H}(0) = \begin{bmatrix} \mathbf{y}(0) & \mathbf{y}(1) & \cdots & \mathbf{y}(N-1) \\ \mathbf{y}(1) & \mathbf{y}(2) & \cdots & \mathbf{y}(N) \\ \vdots & \vdots & \ddots & \vdots \\ \mathbf{y}(M-1) & \mathbf{y}(M) & \cdots & \mathbf{y}(N+M-2) \end{bmatrix}. \tag{8}$$

The number M of block rows of $\mathbf{H}(0)$ is chosen to be greater than N, i.e., $M > N$ and N is greater than the upper bound of the system order p. Using the relation of equation (4), the Hankel matrix can be factored as

$$\mathbf{H}(0) = \mathbf{\Gamma X}, \tag{9}$$

where

$$\mathbf{\Gamma} = \begin{bmatrix} \mathbf{C} \\ \mathbf{CG} \\ \vdots \\ \mathbf{CG}^{M-1} \end{bmatrix} \tag{10}$$

is the observability matrix of the system, and

$$\mathbf{X} = [\mathbf{x}(0) \quad \mathbf{x}(1) \quad \cdots \quad \mathbf{x}(N-1)] \tag{11}$$

is a state matrix. It is noted that $\mathbf{\Gamma}$ has a so-called *shift invariance* structure. Specifically, define two submatrices $\mathbf{\Gamma}_2$ and $\mathbf{\Gamma}_1$ which are obtained from $\mathbf{\Gamma}$ by deleting the first and last block rows, respectively. It is then easy to see that the transition matrix $\mathbf{G}$ is the transformation that maps $\mathbf{\Gamma}_1$ onto $\mathbf{\Gamma}_2$, i.e.,

$$\mathbf{\Gamma}_1 \mathbf{G} = \mathbf{\Gamma}_2. \tag{12}$$

Therefore an estimate of $\mathbf{G}$ can be obtained by solving

$$\mathbf{G} = \mathbf{\Gamma}_1^+ \mathbf{\Gamma}_2, \tag{13}$$

where $(\cdot)^+$ denotes the Moore–Penrose pseudo inverse.

The key of the subspace methods is to extract the observability range space. If the matrix $\bar{\mathbf{\Gamma}}$ has the same range space as that of $\mathbf{\Gamma}$, such a matrix can be written as

$$\bar{\mathbf{\Gamma}} = \mathbf{\Gamma T}^{-1} = \begin{bmatrix} \bar{\mathbf{C}} \\ \bar{\mathbf{C}}\bar{\mathbf{G}} \\ \vdots \\ \bar{\mathbf{C}}\bar{\mathbf{G}}^{M-1} \end{bmatrix}, \tag{14}$$

where $\mathbf{T} \in \mathfrak{R}^{p \times p}$ is some non-singular matrix. Apparently the first block row of $\bar{\mathbf{\Gamma}}$ can be used as $\bar{\mathbf{C}}$. Partitioning $\bar{\mathbf{\Gamma}}$ into $\bar{\mathbf{\Gamma}}_1$ and $\bar{\mathbf{\Gamma}}_2$ as before and invoking equation (13) results in

$$\bar{\mathbf{G}} = \bar{\mathbf{\Gamma}}_1^+ \bar{\mathbf{\Gamma}}_2. \tag{15}$$

There are several methods to retrieve the observability range space. The most commonly used one is the singular value decomposition (SVD) [28]. The popularity of the SVD lies in its numerical stability. This feature is briefly discussed below. The measured responses are corrupted by noise such that

$$\hat{\mathbf{y}}(k) = \mathbf{y}(k) + \mathbf{w}(k), \qquad k = 0, 1, 2, \ldots, L-1, \tag{16}$$

where $\hat{\mathbf{y}}(k)$ is the measured response vector and $\mathbf{w}(k) \in \mathfrak{R}^{n \times 1}$ is a noise vector. Now the general Hankel matrix formed by the noisy responses becomes

$$\hat{\mathbf{H}}(0) = \mathbf{H}(0) + \mathbf{W}(0). \tag{17}$$

Conducting the SVD to $\hat{\mathbf{H}}(0)$ yields

$$\hat{\mathbf{H}}(0) = \mathbf{U\Sigma V}^{\mathrm{H}}, \tag{18}$$

where $(\cdot)^{\mathrm{H}}$ denotes the Hermitian transpose. The matrices $\mathbf{U} \in \mathfrak{R}^{nM \times nM}$ and $\mathbf{V} \in \mathfrak{R}^{N \times N}$ are two orthogonal matrices that are called the left and right singular vector matrices, respectively. The matrix $\mathbf{\Sigma} \in \mathfrak{R}^{nM \times N}$ can be partitioned as

$$\mathbf{\Sigma} = \begin{bmatrix} \mathbf{\Sigma}_r & \mathbf{0} \\ \mathbf{0} & \mathbf{0} \end{bmatrix}, \tag{19}$$

where $\mathbf{\Sigma}_r = \text{diag}\,(\sigma_1, \ldots, \sigma_r)$ with $\sigma_1 \geqslant \cdots \geqslant \sigma_r \geqslant 0$. The number σ_i is called the ith singular value. When the responses are free of noise, r is equal to p. When the data are corrupted by noise, r equals $\min(N, M)$. The SVD of $\hat{\mathbf{H}}(0)$ can be further partitioned as

$$\hat{\mathbf{H}}(0) = \mathbf{U}\mathbf{\Sigma}\mathbf{V}^{\mathrm{H}} = [\mathbf{U}_p \quad \mathbf{U}_w] \begin{bmatrix} \mathbf{\Sigma}_p & \mathbf{0} \\ \mathbf{0} & \mathbf{\Sigma}_w \end{bmatrix} \begin{bmatrix} \mathbf{V}_p^{\mathrm{H}} \\ \mathbf{V}_w^{\mathrm{H}} \end{bmatrix}, \tag{20}$$

where $\mathbf{U}_p$ is formed using the first p columns of $\mathbf{U}$ and $\mathbf{U}_w$ using the rest columns of $\mathbf{U}$. The matrices $\mathbf{V}_p$ and $\mathbf{V}_w$ are formed in a similar manner using $\mathbf{V}$. When the signal-to-noise ratio (SNR) is high or moderate, the diagonal matrix $\mathbf{\Sigma}_p$ contains the first p significantly large singular values and $\mathbf{\Sigma}_w$ the rest, smaller singular values. There can sometimes be real difficulties in determining a ''gap'' between the significantly large singular values and significantly small singular values. Various criteria have been suggested [29]. Using equation (20), the covariance matrix $\hat{\mathbf{H}}\hat{\mathbf{H}}^{\mathrm{H}}$ can be written as

$$\hat{\mathbf{H}}\hat{\mathbf{H}}^{\mathrm{H}} = \mathbf{U}\mathbf{\Sigma}^2\mathbf{U}^{\mathrm{H}} = \mathbf{U}_p\mathbf{\Sigma}_p^2\mathbf{U}_p^{\mathrm{H}} + \mathbf{U}_w\mathbf{\Sigma}_w^2\mathbf{U}_w^{\mathrm{H}}. \tag{21}$$

On the other hand

$$\hat{\mathbf{H}}\hat{\mathbf{H}}^{\mathrm{H}} = \mathbf{H}\mathbf{H}^{\mathrm{H}} + \mathbf{W}\mathbf{H}^{\mathrm{H}} + \mathbf{H}\mathbf{W}^{\mathrm{H}} + \mathbf{W}\mathbf{W}^{\mathrm{H}}. \tag{22}$$

If the measurement noise is zero-mean white noise and uncorrelated with the true response, in the limiting case the following relations exist:

$$\lim_{N\to\infty} \frac{1}{N}\mathbf{H}\mathbf{H}^{\mathrm{H}} = \mathbf{\Gamma}\left(\lim_{N\to\infty} \frac{1}{N}\mathbf{X}\mathbf{X}^{\mathrm{H}}\right)\mathbf{\Gamma}^{\mathrm{H}}, \qquad \lim_{N\to\infty} \frac{1}{N}\mathbf{W}\mathbf{H}^{\mathrm{H}} = \mathbf{0}, \qquad \lim_{N\to\infty} \frac{1}{N}\mathbf{H}\mathbf{W}^{\mathrm{H}} = \mathbf{0},$$

$$\lim_{N\to\infty} \frac{1}{N}\mathbf{W}\mathbf{W}^{\mathrm{H}} = \sigma^2\mathbf{I}, \tag{23}$$

where $\mathbf{X}\mathbf{X}^{\mathrm{H}}$ is the covariance matrix of the state vector, σ^2 is the noise variance, and $\mathbf{I}$ is a unit matrix. Equating equations (21) and (22) in the limit results in

$$\lim_{N\to\infty} \frac{1}{N}\mathbf{U}_p\mathbf{\Sigma}_p^2\mathbf{U}_p^{\mathrm{H}} + \lim_{N\to\infty} \frac{1}{N}\mathbf{U}_w\mathbf{\Sigma}_w^2\mathbf{U}_w^{\mathrm{H}} = \mathbf{\Gamma}\left(\lim_{N\to\infty} \frac{1}{N}\mathbf{X}\mathbf{X}^{\mathrm{H}}\right)\mathbf{\Gamma}^{\mathrm{H}} + \sigma^2\mathbf{I}. \tag{24}$$

The above analysis indicates that, for a sufficiently long data length N, the following approximation holds:

$$\mathbf{U}_p\mathbf{\Sigma}_p^2\mathbf{U}_p^{\mathrm{H}} \approx \mathbf{\Gamma}(\mathbf{X}\mathbf{X}^{\mathrm{H}})\mathbf{\Gamma}^{\mathrm{H}}, \tag{25}$$

which also shows that $\mathbf{U}_p$ forms an orthonormal basis for the observability range space, i.e., $\bar{\mathbf{\Gamma}} \approx \mathbf{U}_p$.

Among other subspace extraction algorithms, the classical Gram–Schmidt (CGS) orthonormalization [28] is worth mentioning. This method was used to develop a recursive form of the ERA algorithm in reference [23]. The Gram–Schmidt orthonormalization of the columns of $\hat{\mathbf{H}}$ produces a matrix factorization in the form

$$\hat{\mathbf{H}} = \mathbf{Q}\mathbf{R}, \tag{26}$$

where $\mathbf{Q} \in \mathfrak{R}^{nM \times nM}$ is orthogonal and $\mathbf{R} \in \mathfrak{R}^{nM \times N}$ is upper triangular. The first p columns of $\mathbf{Q}$ can be used as the observability range space. The main advantage of the method is that

the construction of $\mathbf{Q}$ and determination of the system order p are done recursively such that the computer storage and time are drastically reduced. However, in terms of numerical sensitivity to the noise, the SVD is better than the classical Gram–Schmidt method.

3. IDENTIFICATION OF TIME-VARYING SYSTEMS

The state space representation of a $p/2$-degree-of-freedom LTV and freely vibrating system is given by

$$\dot{\mathbf{x}}(t) = \mathbf{A}(t)\mathbf{x}(t),\ \mathbf{x}(0), \qquad \mathbf{y}(t) = \mathbf{C}(t)\mathbf{x}(t), \tag{27}$$

where the parameter matrices $\mathbf{A}(t)$ and $\mathbf{C}(t)$ are time dependent. The following assumptions are used in the study. The elements of $\mathbf{A}(t)$ and $\mathbf{C}(t)$ are bounded and have a finite number of the first order discontinuous points within the interval of interest. The system is asymptotically stable, i.e., $\mathbf{y}(t)$ approaches zero when t approaches infinity for any initial condition $\mathbf{x}(0)$. The state dimension p is constant. The system is observable.

The corresponding discrete-time space state model becomes

$$\mathbf{x}(k+1) = \mathbf{G}(k+1, k)\mathbf{x}(k), \mathbf{x}(0); \qquad \mathbf{y}(k) = \mathbf{C}(k)\mathbf{x}(k), \tag{28}$$

where $\mathbf{G}(k+1, k)$ is referred to as varying state transition matrix. The observability of LTV systems requires that $\mathbf{G}(k+1, k)$ be non-singular at any moment k [7]. Unlike time-invariant systems, in general, no closed-form of the varying transition matrix $\mathbf{G}(k+1, k)$ is known. Two important properties of $\mathbf{G}(k+1, k)$ are

$$\mathbf{G}(k+1, h) = \mathbf{G}(k+1, k)\mathbf{G}(k, h),\ k > h; \qquad \mathbf{G}(h, h) = \mathbf{I}. \tag{29}$$

The solution of equation (28) is given by

$$\mathbf{y}(k) = \mathbf{C}(k)\mathbf{G}(k, 0)\mathbf{x}(0). \tag{30}$$

For LTV systems, the similarity transformation matrix is no longer constant. If non-singular matrices $\mathbf{T}(k+1)$ and $\mathbf{T}(k) \in \mathfrak{R}^{p \times p}$ exist, the similarity transformation is defined as

$$\bar{\mathbf{G}}(k+1, k) = \mathbf{T}(k+1)\mathbf{G}(k+1, k)\mathbf{T}^{-1}(k), \qquad \bar{\mathbf{C}}(k) = \mathbf{C}(k)\mathbf{T}^{-1}(k), \tag{31}$$

where $\bar{\mathbf{G}}(k+1, k)$ and $\bar{\mathbf{C}}(k)$ are another realization of the system. It should be noted that, although $\bar{\mathbf{G}}(k+1, k)$ preserves the boundedness and stability of the transformed system, normally, $\bar{\mathbf{G}}(k+1, k)$ and $\mathbf{G}(k+1, k)$ do not share the same eigenvalues. One of the particular interests of this study is to find the eigenvalues of $\mathbf{G}(k+1, k)$. Therefore, it is suggested that a matrix be introduced; defined as

$$\tilde{\mathbf{G}}(k+1, k) = \mathbf{T}(k)\mathbf{G}(k+1, k)\mathbf{T}^{-1}(k). \tag{32}$$

Apparently the matrix $\tilde{\mathbf{G}}(k+1, k)$ guarantees the invariability of the eigenvalues. In general, the identification of $\bar{\mathbf{C}}(k)$, $\bar{\mathbf{G}}(k+1, k)$, and $\tilde{\mathbf{G}}(k+1, k)$ cannot be accomplished through the data from a single experiment. In what follows, this problem is approached by the so-called ensemble method.

3.1. USE OF AN ENSEMBLE OF RESPONSE SEQUENCES

Assume that N experiments have been conducted on the system whose parameters undergo the same variation. The noise-free responses from the jth experiment are represented by $\mathbf{y}_j(k)$ where $j = 1, 2, \ldots, N$ and $k = 0, 1, 2, \ldots, L-1$. A general block Hankel matrix is formed using the M successive responses of N experiments:

$$\mathbf{H}(k) = \begin{bmatrix} \mathbf{y}_1(k) & \mathbf{y}_2(k) & \cdots & \mathbf{y}_N(k) \\ \mathbf{y}_1(k+1) & \mathbf{y}_2(k+1) & \cdots & \mathbf{y}_N(k+1) \\ \vdots & \vdots & \ddots & \vdots \\ \mathbf{y}_1(k+M-1) & \mathbf{y}_2(k+M-1) & \cdots & \mathbf{y}_N(k+M-1) \end{bmatrix}. \tag{33}$$

$\mathbf{H}(k)$ can be factored as

$$\mathbf{H}(k) = \mathbf{\Gamma}(k)[\mathbf{x}_1(k) \quad \mathbf{x}_2(k) \quad \mathbf{x}_3(k) \quad \cdots \quad \mathbf{x}_N(k)], \tag{34}$$

where the observability matrix $\mathbf{\Gamma}(k)$ is of the form

$$\mathbf{\Gamma}(k) = \begin{bmatrix} \mathbf{C}(k) \\ \mathbf{C}(k+1)\mathbf{G}(k+1,k) \\ \mathbf{C}(k+2)\mathbf{G}(k+2,k) \\ \vdots \\ \mathbf{C}(k+M-1)\mathbf{G}(k+M-1,k) \end{bmatrix}. \tag{35}$$

Its corresponding range space becomes

$$\bar{\mathbf{\Gamma}}(k) = \mathbf{\Gamma}(k)\mathbf{T}^{-1}(k) = \begin{bmatrix} \bar{\mathbf{C}}(k) \\ \bar{\mathbf{C}}(k+1)\bar{\mathbf{G}}(k+1,k) \\ \bar{\mathbf{C}}(k+2)\bar{\mathbf{G}}(k+2,k) \\ \vdots \\ \bar{\mathbf{C}}(k+M-1)\bar{\mathbf{G}}(k+M-1,k) \end{bmatrix}. \tag{36}$$

Apparently the shift invariance property no longer exists in a single observability matrix $\mathbf{\Gamma}(k)$ or its range space $\bar{\mathbf{\Gamma}}(k)$. To extract $\bar{\mathbf{G}}(k+1,k)$, a successive Hankel matrix $\mathbf{H}(k+1)$ is formed using the $k+1$ to $k+M$ successive responses of N experiments. The matrix $\mathbf{H}(k+1)$ can be factored as

$$\mathbf{H}(k+1) = \mathbf{\Gamma}(k+1)\,[\mathbf{x}_1(k+1) \quad \mathbf{x}_2(k+1) \quad \mathbf{x}_3(k+1) \quad \cdots \quad \mathbf{x}_N(k+1)], \tag{37}$$

where $\mathbf{\Gamma}(k+1)$ has a similar form as equation (35) and its range space $\bar{\mathbf{\Gamma}}(k+1)$ is given by

$$\bar{\mathbf{\Gamma}}(k+1) = \mathbf{\Gamma}(k+1)\mathbf{T}^{-1}(k+1) = \begin{bmatrix} \bar{\mathbf{C}}(k+1) \\ \bar{\mathbf{C}}(k+2)\bar{\mathbf{G}}(k+2,k+1) \\ \bar{\mathbf{C}}(k+3)\bar{\mathbf{G}}(k+3,k+1) \\ \vdots \\ \bar{\mathbf{C}}(k+M)\bar{\mathbf{G}}(k+M,k+1) \end{bmatrix}. \tag{38}$$

Now let $\bar{\mathbf{\Gamma}}_1(k+1)$ be the first $M-1$ block rows of $\bar{\mathbf{\Gamma}}(k+1)$ and $\bar{\mathbf{\Gamma}}_2(k)$ the last $M-1$ block rows of $\bar{\mathbf{\Gamma}}(k)$. The matrix $\bar{\mathbf{G}}(k+1,k)$ can be found by

$$\bar{\mathbf{G}}(k+1,k) = [\bar{\mathbf{\Gamma}}_1(k+1)]^{+}\bar{\mathbf{\Gamma}}_2(k). \tag{39}$$

In a practical implementation, the SVD of these two successive Hankel matrices formed by the noisy data results in $\hat{\mathbf{H}}(k) = \mathbf{U}(k)\mathbf{\Sigma}(k)\mathbf{V}(k)^{\mathrm{H}}$ and $\hat{\mathbf{H}}(k+1) = \mathbf{U}(k+1)\mathbf{\Sigma}(k+1)\mathbf{V}(k+1)^{\mathrm{H}}$. Let $\mathbf{U}_p(k) \approx \bar{\mathbf{\Gamma}}(k)$ and $\mathbf{U}_p(k+1) \approx \bar{\mathbf{\Gamma}}(k+1)$. Forming $\mathbf{U}_{p1}(k+1)$ and $\mathbf{U}_{p2}(k)$ as before and invoking equation (39) results in

$$\bar{\mathbf{G}}(k+1,k) = [\mathbf{U}_{p1}(k+1)]^{+}\mathbf{U}_{p2}(k) = \mathbf{T}(k+1)\mathbf{G}(k+1,k)\mathbf{T}^{-1}(k). \tag{40}$$

However, because $\mathbf{T}(k)$ and $\mathbf{T}(k+1)$ are unavailable, the exact solution of $\tilde{\mathbf{G}}(k+1,k)$ cannot be found. Instead an approximate solution for $\tilde{\mathbf{G}}(k+1,k)$ is proposed as follows. If $n \geqslant p$, let the first block row of $\mathbf{U}_p(k)$ be $\mathbf{F}(k)$ and the first block row of $\mathbf{U}_p(k+1)$ be $\mathbf{F}(k+1)$. It is easy to prove that the following relation exists

$$\mathbf{F}^+(k)\mathbf{F}(k+1) = \mathbf{T}(k)\,[\mathbf{C}^{\mathrm{T}}(k)\mathbf{C}(k)]^{-1}\mathbf{C}^{\mathrm{T}}(k)\mathbf{C}(k+1)\mathbf{T}^{-1}(k+1). \tag{41}$$

To ensure the existence of $\mathbf{F}^+(k)$, $\mathbf{C}(k)$ must have full column rank. When $n < p$, i.e., rank $(\mathbf{C}(k)) < p$, a remedy for this problem is given in Appendix A. Premultiplying $\bar{\mathbf{G}}(k+1,k)$ with $\mathbf{F}^+(k)\mathbf{F}(k+1)$ yields

$$\tilde{\mathbf{G}}(k+1,k) \approx \mathbf{F}^+(k)\mathbf{F}(k+1)\bar{\mathbf{G}}(k+1,k). \tag{42}$$

Apparently, the accuracy of the above approximation depends on the variability of $\mathbf{C}(k)$.

A computing procedure is summarized as follows: To identify $\bar{\mathbf{C}}(i)$, $\bar{\mathbf{G}}(i+1,i)$, and $\tilde{\mathbf{G}}(i+1,i)$, $i = 0, 1, \ldots, k_f$, start with $i = 0$ and carry out the following:

(1) Form $\hat{\mathbf{H}}(i)$. Conduct the SVD on $\hat{\mathbf{H}}(i)$ to obtain $\mathbf{U}(i)$. Form $\mathbf{U}_{p2}(i)$ and $\mathbf{F}(i)$.

(2) Form $\hat{\mathbf{H}}(i+1)$. Conduct the SVD on $\hat{\mathbf{H}}(i+1)$ to obtain $\mathbf{U}(i+1)$. Form $\mathbf{U}_{p1}(i+1)$ and $\mathbf{F}(i+1)$.

(3) Let $\mathbf{F}(i)$ be $\bar{\mathbf{C}}(i)$. Use $\mathbf{U}_{p1}(i)$ and $\mathbf{U}_{p2}(i+1)$ in equation (40) to find $\bar{\mathbf{G}}(i+1,i)$. Use $\mathbf{F}(i)$, $\mathbf{F}(i+1)$, and $\bar{\mathbf{G}}(i+1,i)$ in equation (42) to find $\tilde{\mathbf{G}}(i+1,i)$.

(4) Store $\mathbf{U}(i+1)$ in $\mathbf{U}(i)$. If $i < k_f - 1$, increase i by 1 and go to Step 2.

3.2. USE OF A SINGLE RESPONSE SEQUENCE

If only a single response sequence is available, the identification is possible in two special cases, that is, periodically varying systems and slowly varying systems. In what follows, these two cases are addressed briefly.

3.2.1. *Periodically varying systems*

Assume that $P\Delta t$ is the period of the parameter variation. The transition matrix of the periodic system satisfies [30]

$$\mathbf{G}(P+k+1, P+k) = \mathbf{G}(k+1,k). \tag{43}$$

The transformation matrix is also periodic, i.e.,

$$\mathbf{T}(P+k) = \mathbf{T}(k). \tag{44}$$

If the Hankel matrix is formed as

$$\mathbf{H}(k) = \begin{bmatrix} \mathbf{y}(k) & \mathbf{y}(P+k) & \cdots & \mathbf{y}((N-1)P+k) \\ \mathbf{y}(k+1) & \mathbf{y}(P+k+1) & \cdots & \mathbf{y}((N-1)P+k+1) \\ \vdots & \vdots & \ddots & \vdots \\ \mathbf{y}(k+M-1) & \mathbf{y}(P+k+M-1) & \cdots & \mathbf{y}((N-1)P+k+M-1) \end{bmatrix}, \tag{45}$$

it can be factored as

$$\mathbf{H}(k) = \mathbf{\Gamma}(k)\,[\mathbf{x}(k) \quad \mathbf{x}(P+k) \quad \mathbf{x}(2P+k) \quad \cdots \quad \mathbf{x}((N-1)P+k)], \tag{46}$$

where $\mathbf{\Gamma}(k)$ has the same form as equation (35). Thus, the discussion following (35) in the above subsection is also applicable here.

3.2.2. *Slowly varying systems*

If the change in the parameters over any block of N time instants is small, the following $M \times N (M > N)$ block Hankel matrix is constructed:

$$\mathbf{H}(k) = \begin{bmatrix} \mathbf{y}(k) & \mathbf{y}(k+1) & \cdots & \mathbf{y}(k+N-1) \\ \mathbf{y}(k+1) & \mathbf{y}(k+2) & \cdots & \mathbf{y}(k+N) \\ \vdots & \vdots & \ddots & \vdots \\ \mathbf{y}(k+M-1) & \mathbf{y}(k+M) & \cdots & \mathbf{y}(k+N+M-2) \end{bmatrix}. \tag{47}$$

The columns of the above matrix can be factored as

$$\begin{bmatrix} \mathbf{y}(k+j) \\ \mathbf{y}(k+j+1) \\ \vdots \\ \mathbf{y}(k+j+M-1) \end{bmatrix} = \mathbf{\Gamma}(k+j)\mathbf{x}(k+j), \qquad j = 0, 1, 2, \ldots, N-1, \tag{48}$$

where

$$\mathbf{\Gamma}(k+j) = \begin{bmatrix} \mathbf{C}(k+j) \\ \mathbf{C}(k+j+1)\mathbf{G}(k+j+1, k+j) \\ \vdots \\ \mathbf{C}(k+j+M-1)\mathbf{G}(k+j+M-1, k+j) \end{bmatrix}, \qquad j = 0, 1, 2, \ldots, N-1. \tag{49}$$

If the system is slowly varying, the following approximate relation can be justified:

$$\begin{aligned} &\mathbf{G}(k+1, k) \approx \mathbf{G}(k+2, k+1) \approx \cdots \approx \mathbf{G}(k+N, k+N-1), \\ &\mathbf{C}(k+1, k) \approx \mathbf{C}(k+2, k+1) \approx \cdots \approx \mathbf{C}(k+N, k+N-1), \end{aligned} \tag{50}$$

which means

$$\mathbf{\Gamma}(k) \approx \mathbf{\Gamma}(k+1) \approx \cdots \approx \mathbf{\Gamma}(k+N-1). \tag{51}$$

Thus, the Hankel matrix may be approximately factored as

$$\mathbf{H}(k) \approx \mathbf{\Gamma}(k) [\mathbf{x}(k) \quad \mathbf{x}(k+1) \quad \mathbf{x}(k+2) \quad \cdots \quad \mathbf{x}(k+N-1)]. \tag{52}$$

Therefore, the algorithm presented in the previous subsection can be also applied here in a similar manner.

3.3. DATA LENGTH L, COLUMN NUMBER N, AND BLOCK ROW NUMBER M

The total data length L is determined by the final desired transition matrix $\tilde{\mathbf{G}}(k_f + 1, k_f)$. In the case of the ensemble data sequences, $L = k_f + M$. In the case of periodic systems, $L = (N-1)P + k_f + M$. In the case of slowly varying systems, $L = k_f + N + M - 1$. From the noise reduction point of view, N is desired to be as large as possible in order to improve the estimation accuracy. However what is the minimum number of N? In the case of the ensemble data sequences, selection of N or number of experiments should ensure that the rank of the Hankel matrix is greater than the upper bound of the system order p. When a single data sequence is used, a larger N means a longer data length. For slowly varying systems, to select N, several factors should be considered such as the upper bound of the system order, the system variability, and the noise reduction by the SVD. In general, a lower system variability allows to use a larger N. On the other hand, a larger

N may not always improve the estimate accuracy. When multiple experiments are used, a larger N makes it more difficult to ensure the column independence of the Hankel matrix. When a single data sequence is used, a long data length causes a poor signal-to-noise ratio near the tail of the record due to a quicker decay of higher modes. After N is chosen, in general, M is selected to be greater than N. A simple reason is to guarantee that the rank of $\hat{\mathbf{H}}$ is greater than the upper bound of the system order.

4. EIGENVALUES OF THE VARYING TRANSITION MATRIX

Modal parameters have been used to characterize the global properties of LTI systems. As pointed out previously, the modal parameters of LTI systems are related to the eigenvalues of the transition matrix $\bar{\mathbf{G}}$. However, for time-varying systems, the eigenvalues and eigenvectors of the varying transition matrix $\mathbf{G}(k+1,k)$ or $\tilde{\mathbf{G}}(k+1,k)$ no longer have such physical interpretation. Since the transition matrix $\tilde{\mathbf{G}}(k+1,k)$ is non-singular, its eigendecomposition exists, i.e.,

$$\tilde{\mathbf{G}}(k+1,k) = \mathbf{V}(k+1,k)\mathbf{\Lambda}(k+1,k)\mathbf{V}^{-1}(\mathrm{k}+1,\mathrm{k}), \tag{53}$$

where, in analogy to LTI systems, $\mathbf{V}(k+1,k)$ is referred to as the pseudoeigenvector matrix and $\mathbf{\Lambda}(k+1,k) = \mathrm{diag}\,(\lambda_1(k+1,k),\ldots,\lambda_p(k+1,k))$ is referred to as the pseudoeigenvalue matrix. Because the elements of the $\tilde{\mathbf{G}}(k+1,k)$ are real, the complex eigenvalues occur in pairs. If the ith eigenvalue is complex, then the following relation can be employed:

$$\lambda_i(k+1,k) = \lambda^*_{i+p/2}(k+1,k) = \exp(-\delta_i(k+1,k)\Delta t + \mathrm{j}\omega_{di}(k+1,k)\Delta t), \tag{54}$$

where $\delta_i(k+1,k)$ and $\omega_{di}(k+1,k)$ are referred to as the ith pseudodamping factor and pseudodamped natural frequency, respectively. The use of the pseudomodal parameters makes it possible to discuss the properties of varying systems in terms of modal parameters. For example, the asymptotic stability requires that the eigenvalues of $\tilde{\mathbf{G}}(k+1,k)$ be within the unit circle, i.e., $\delta_i(k+1,k) \geqslant 0$. If some of the eigenvalues are outside of the unit circle, the system becomes unstable or temporarily unstable. If the system undergoes a limited time variation, that is, from an old invariant status to a new invariant status, the pseudomodal parameters constitute a transition from the old modal parameters to the new modal parameters. If the system is a slowly varying one, the eigenvalues of $\tilde{\mathbf{G}}(k+1,k)$ can be approximated by the so-called frozen poles that are the first order approximation of the zeros of Zadeh's transfer function [31]. The eigenvalues of the transition matrix over a duration of time can also be used to describe the properties of the varying system over this period. For the transition matrix from the moment k to the moment $k+i$, an eigendecomposition is written as

$$\tilde{\mathbf{G}}(k+i,k) = \mathbf{V}(k+i,k)\mathbf{\Lambda}(k+i,k)\mathbf{V}^{-1}(k+i,k). \tag{55}$$

In a similar manner, a pair of conjugate complex eigenvalues can be expressed as

$$\lambda_i(k+i,k) = \lambda^*_{i+p/2}(k+i,k) = \exp(-\delta_i(k+i,k)\Delta t + \mathrm{j}\omega_{di}(k+i,k)\Delta t). \tag{56}$$

In the case of a periodic system, according to Floquet theory, the transition matrix over a period is a constant matrix, i.e.,

$$\mathbf{G}(k+P,k) = \mathbf{\Phi} \text{ or } \tilde{\mathbf{G}}(k+P,k) = \tilde{\mathbf{G}}(k+P,k) = \tilde{\mathbf{\Phi}}, \tag{57}$$

where $\mathbf{\Phi}$ or $\tilde{\mathbf{\Phi}}$ is a constant matrix. Therefore, the eigenvalues of $\mathbf{G}(k+P,k)$ or $\tilde{\mathbf{G}}(k+P,k)$ are independent of k. These eigenvalues have been used to determine the asymptotic stability of a periodic system in [30].

5. AN ILLUSTRATIVE EXAMPLE

To illustrate the algorithm developed above, an example is presented in this section. Shown in Figure 1, a planar two-link manipulator subjected to a varying end force is used as the example. The links are assumed to be rigid. The elasticity of joints 1 and 2 is represented by two constant rotational springs k_1 and k_2. The system damping is assumed to be viscous, constant, and concentrated at the joints. The damping coefficients at joints 1 and 2 are d_1 and d_2, respectively. The angles φ_1 and φ_2 denote the angular positions of the links relative to the x-axis. A time-varying force $f(t)$ acts at the free end of the second link, making the angle φ_3 with the x-axis. φ_3 is assumed to be constant during vibration for simplicity. A detailed dynamic model and the stability of such system can be found in reference [10]. For the sake of simplicity, it is assumed that the links of the manipulator are uniform cylinders of equal length l and mass m. When an initial disturbance is applied, the links vibrate around their equilibrium positions φ_{10} and φ_{20}. The actual angular position of the links become $\varphi_1 = \varphi_{10} + \varphi_{11}$ and $\varphi_2 = \varphi_{20} + \varphi_{21}$. With the assumption of small angular vibrations, a linearized model for the system under the free vibration is defined by the matrix equation

$$\mathbf{M}\ddot{\varphi} + \mathbf{D}\dot{\varphi} + \mathbf{K}(t)\varphi = \mathbf{0}, \tag{58}$$

where

$$\mathbf{M} = \begin{bmatrix} a_1 & a_2 \cos(\varphi_{10} - \varphi_{20}) \\ a_2 \cos(\varphi_{10} - \varphi_{20}) & a_3 \end{bmatrix}, \qquad \mathbf{D} = \begin{bmatrix} d_1 + d_2 & -d_2 \\ -d_2 & d_2 \end{bmatrix},$$

$$\mathbf{K}(t) = \begin{bmatrix} k_1 + k_2 - a_4 \sin\varphi_{10} - f(t)l\cos(\varphi_{10} - \varphi_3) & -k_2 \\ -k_2 & k_2 - a_5 \sin\varphi_{20} - f(t)l\cos(\varphi_{20} - \varphi_3) \end{bmatrix},$$

$$\varphi = [\varphi_{11} \quad \varphi_{21}]^{\mathrm{T}},\ a_1 = 4ml^2/3,\ a_2 = ml^2/2,\ a_3 = ml^2/3,\ a_4 = 3ml^2g/2,\ a_5 = ml^2g/2.$$

If the state vector is defined as $\mathbf{x} = [\dot{\varphi}^{\mathrm{T}}, \varphi^{\mathrm{T}}]^{\mathrm{T}}$, then the state space model of equation (27) is obtained and the parameter matrix $\mathbf{A}(t)$ is of the form

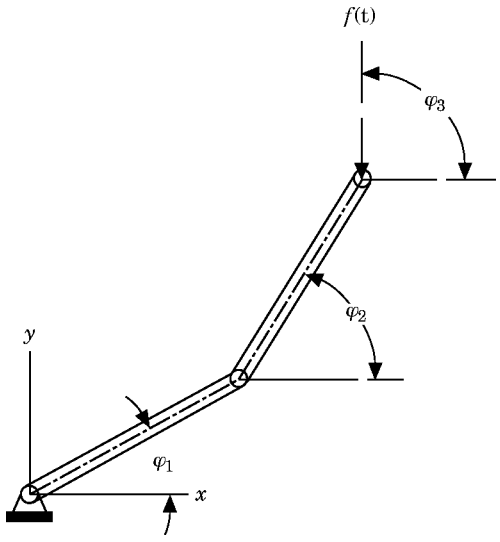

Figure 1. A two-link manipulator subjected to a varying force $f(t)$ at its free end.

$$\mathbf{A}(t) = \begin{bmatrix} \mathbf{0} & \mathbf{M} \\ \mathbf{M} & \mathbf{D} \end{bmatrix}^{-1} \begin{bmatrix} -\mathbf{M} & \mathbf{0} \\ \mathbf{0} & \mathbf{K}(t) \end{bmatrix}. \tag{59}$$

In the simulation, the following numerical quantities were used: the length $l = 1$ m, the mass $m = 1$ kg, the stiffness $k_1 = k_2 = 80$ Nm/rad, $d_1 = d_2 = 0{\cdot}8$ Nms/rad, the force application angle $\varphi_3 = 90^\circ$. The testing configuration of the manipulator was set at $\varphi_{10} = 0^\circ$ and $\varphi_{20} = 90^\circ$. It was assumed that the system order $p = 4$ was known and that the state variables were directly available, i.e., $\mathbf{C} = \mathbf{I}$ or $\mathbf{y} = \mathbf{x}$. The signal-to-noise ratio (SNR) is defined as

$$\text{SNR} = \sigma_{y_i}/\sigma_i, \qquad i = 1, 2, 3, 4, \tag{60}$$

where σ_{y_i} denotes the standard deviation of the ith response and σ_i is the standard deviation of the noise added to the ith response. In the actual implementation, first equation (58) was numerically integrated using the Runge–Kutta method to find $y_i(k)$. Then σ_{y_i} was found. Using a given SNR, σ_i was determined by equation (60). Finally a standard Gaussian white noise with a unit standard deviation was generated, multiplied by the value σ_i and added to $y_i(k)$ to produce the measured response $\hat{y}_i(k) = y_i(k) + w_i(k)$. The true transition matrices of the system under study were evaluated numerically using the method given in Appendix A.

5.1. THE USE OF AN ENSEMBLE OF RESPONSES

To test the algorithm using an ensemble of responses, let the force vary in a piecewise pattern, that is,

$$f(t) = \begin{cases} f_0 & 0 \leqslant t \leqslant 0{\cdot}5, \\ f_0 - \Delta f \sin(\pi(t - 0{\cdot}5)/2\tau), & 0{\cdot}5 \leqslant t \leqslant \tau + 0{\cdot}5, \\ f_0 - \Delta f, & \tau + 0{\cdot}5 < t, \end{cases} \tag{61}$$

where $f_0 = 20$ N and $\Delta f = 10$ N. The damped natural frequencies are $\omega_{d1} = 4{\cdot}5304$ rad/s, $\omega_{d2} = 16{\cdot}271$ rad/s for the period of $0 \leqslant t \leqslant 0{\cdot}5$ and $\omega_{d1} = 5{\cdot}6459$ rad/s, $\omega_{d2} = 16{\cdot}834$ rad/s for the period of $\tau + 0{\cdot}5 < t$. Different experiments were obtained by disturbing the system using different initial conditions. The 12 initial conditions used in the simulation are given as

$$[\mathbf{x}_1(0), \mathbf{x}_2(0), \ldots, \mathbf{x}_{12}(0)] = \begin{bmatrix} 1 & 0 & 0 & 0 & -1{\cdot}5 & 2 & 0 & 0 & 0 & 1 & 0 & 0 \\ 0 & -1 & 0 & 0 & 0{\cdot}5 & -1 & 0 & 0 & -1 & 0 & 0 & 0 \\ 0 & 0 & -0{\cdot}1 & 0 & 0 & 0 & 0 & -0{\cdot}1 & 0 & 0 & 0{\cdot}5 & -0{\cdot}1 \\ 0 & 0 & 0 & 0{\cdot}1 & 0 & 0 & 0{\cdot}1 & 0 & 0 & 0 & -0{\cdot}15 & 0{\cdot}2 \end{bmatrix}. \tag{62}$$

The initial conditions have been chosen to be independent of one another. The time interval was chosen to be $\Delta t = 0{\cdot}04$ s. In what follows, the results of estimation is presented in two ways: an average $\bar{\omega}_{di}(k)$ of 10 estimates of the pseudodamped natural frequencies at instant k and the sum S_i of the standard deviation of the estimated values

$$\bar{\omega}_{di}(k) = \frac{1}{10} \sum_{j=1}^{10} \omega_{dij}(k), \qquad S_i = \sum_{k=0}^{l-1} \sigma_i(k), \qquad i = 1, 2, \tag{63}$$

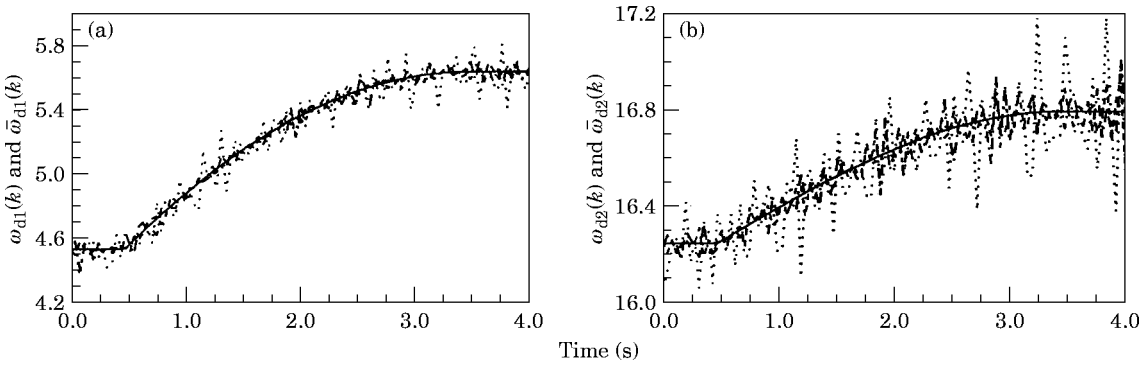

Figure 2. The estimated pseudodamped natural frequencies and the true values when the system undergoes a piecewise variation with $\tau = 3$ s. (a) ——, true $\omega_{d1}(k)$; · · · · · , $\bar{\omega}_{d1}(k)$ SNR = 50; ·–·–·–· , $\bar{\omega}_{d1}(k)$ SNR = 100; - - - -, $\bar{\omega}_{d1}(k)$ SNR = 150; (b) ——, true $\omega_{d2}(k)$; · · · · · , $\bar{\omega}_{d2}(k)$ SNR = 50; ·–·–·–· , $\bar{\omega}_{d2}(k)$ SNR = 100; - - - -, $\bar{\omega}_{d2}(k)$ SNR = 150.

where the standard deviation of the estimated pseudodamped natural frequencies is defined as

$$\sigma_i(k) = \sqrt{\frac{1}{10}\sum_{j=1}^{10}[\omega_{dij}(k) - \bar{\omega}_{di}(k)]^2}, \qquad i = 1, 2. \tag{64}$$

First the tracking ability and the robustness of the algorithm are shown in Figures 2(a) and (b). Figure 2(a) shows a comparison of the estimated first pseudo damped natural frequencies with the true values. Figure 2(b) gives a comparison of the estimated second damped natural frequencies with the true values. In the computation, τ was chosen to be 3 s. The first six initial conditions in equation (62) were used to produce six experiments, i.e., $N = 6$. The block row number M was chosen to be 10. It is noted that the estimated $\bar{\omega}_{d1}(k)$ and $\bar{\omega}_{d2}(k)$ follow the variation of the true values well. The fluctuation of the estimated values reduces when SNR increases. To further demonstrate the capability of tracking a fast variation, Figures 3(a) and (b) show a comparison of the estimated damped natural frequencies and the true values when τ was shortened to be 1 s. Again the similar tracking ability and robustness are observed.

Figures 4(a) and (b) are used to show the effects of different N s. The index S_i defined above is employed as a condensed indicator of the estimate accuracy. A smaller S_i

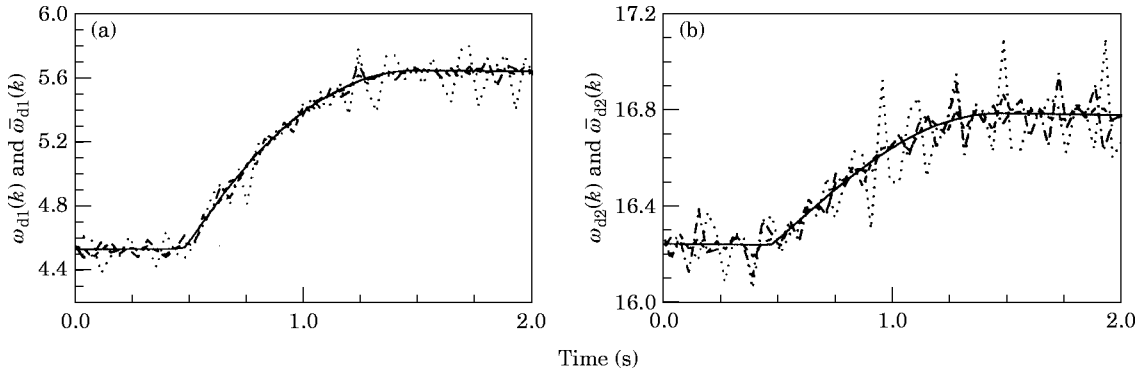

Figure 3. The estimated pseudodamped natural frequencies and the true values when the system undergoes a piecewise variation with $\tau = 1$ s. Key for (a) and (b) as for Figure 2.

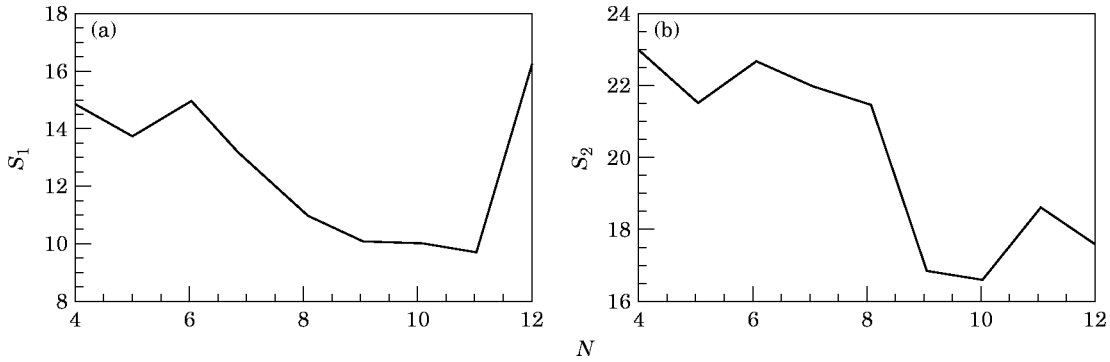

Figure 4. Relation between the index S_i defined in equation (63) and N. (a) S_1 versus N, (b) S_2 versus N.

corresponds to a smaller fluctuation of the estimated values or a more accurate estimate. The results in Figures 4(a) and (b) were obtained using the same conditions as those for Figures 2(a) and (b) except that SNR was fixed to be 100 and N experiments were generated using the first N initial conditions in equation (62). It is noted that the change of S_i is not monotonic. An increase of N first results in a decrease of S_i and then a slight increase of S_i. Such a behavior indicates that a large N does not necessarily improve the estimate accuracy. An explanation for this phenomenon is that a large N is likely to cause the column dependence of the Hankel matrix if the initial conditions are not chosen properly. The effects of altering M were also investigated. It has been noted that varying M has little influence on S_i.

A comparison of the SVD method and the CGS method is given in Figures 5(a) and (b). The conditions for Figures 5(a) and (b) were the same as those for Figures 2(a) and (b). Apparently the estimate accuracy of the SVD is better than that of the CGS method. However, the CGS method significantly reduces the computational burden. This feature becomes more attractive when the system order is large.

5.2. ESTIMATION OF A PERIODICALLY VARYING SYSTEM

To create a periodic system, let the force follow a sinusoidal variation, i.e.,

$$f(t) = f_0 - \Delta f \sin(2\pi t/\tau), \tag{65}$$

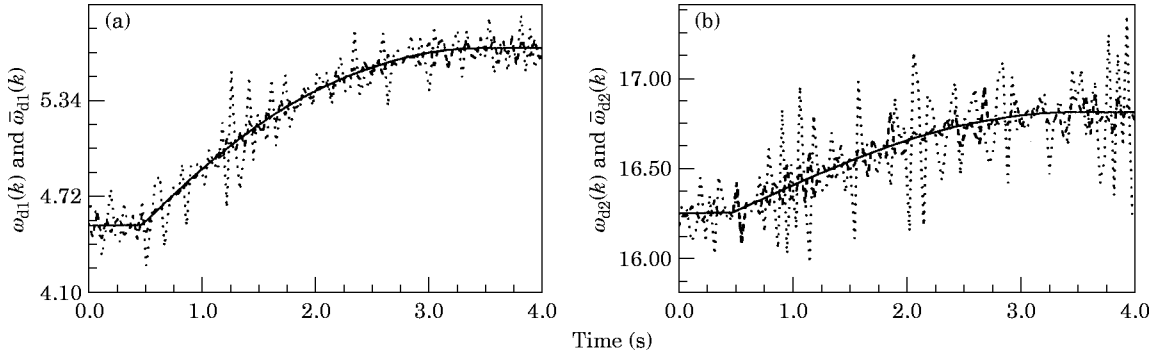

Figure 5. Comparison of the estimates using the SVD and the estimates using the CGS. (a) ——, true $\omega_{d1}(k)$; - - - -, $\bar{\omega}_{d1}(k)$ using the SVD; · · · · · , $\bar{\omega}_{d1}(k)$ using the CGS; (b) ——, true $\omega_{d2}(k)$; - - - , $\bar{\omega}_{d2}(k)$ using the SVD; · · · · · , $\bar{\omega}_{d2}(k)$ using the CGS.

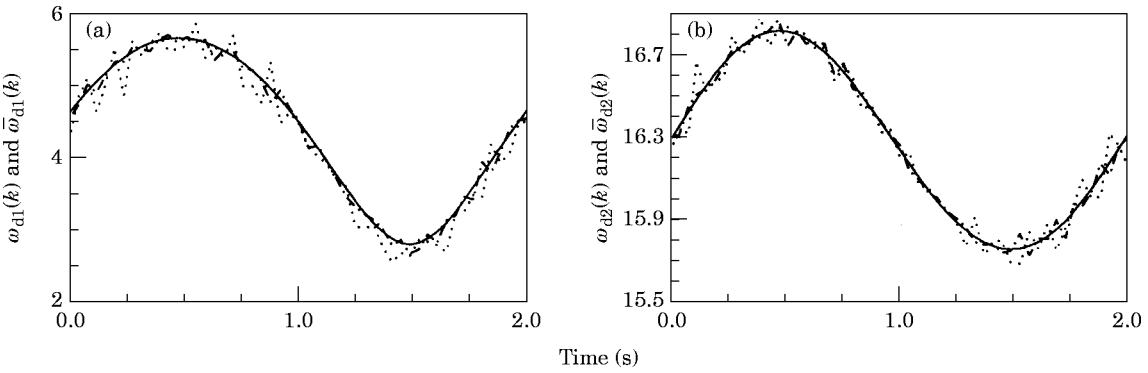

Figure 6. The estimated pseudodamped natural frequencies and the true values when the system undergoes a periodic variation with $\tau = 2$ s. (a) ——, true $\omega_{d1}(k)$; · · · · ·, $\bar{\omega}_{d1}(k)$ SNR = 50; - - - -, $\bar{\omega}_{d1}(k)$ SNR = 100; (b) ——, true $\omega_{d2}(k)$, · · · · ·, $\bar{\omega}_{d2}(k)$ SNR = 50; - - - -, $\bar{\omega}_{d2}(k)$ SNR = 100.

where $f_0 = 20$ N and $\Delta f = 10$ N. The variation period was $\tau = 2$ s, i.e., $P = 50$. A response series was generated by an initial condition $\mathbf{x}(0) = [0{\cdot}1 \; -0{\cdot}1 \; 0 \; 0]^{\mathrm{T}}$. The Hankel matrix was formed by choosing $M = 10$ and $N = 6$. Figures 6(a) and (b) compare the averages of the estimated pseudo damped natural frequencies with the true values. It is seen that the estimated $\bar{\omega}_{d1}(k)$ and $\bar{\omega}_{d2}(k)$ track the parameter variation closely. As another way to demonstrate the estimated results, the eigenvalues of $\tilde{\mathbf{G}}(50, 0)$ are shown in Figures 7 and 8. Figures 7(a) and (b) give 20 estimates of the first eigenvalue when $N = 6$ and $N = 12$, respectively. Figures 8(a) and (b) give 20 estimates of the second eigenvalue when $N = 6$ and $N = 12$, respectively. It is seen that, with an increase of N, the estimated eigenvalues become closer to the true values.

5.3. ESTIMATION OF A SLOWLY VARYING SYSTEM

To create a slowly varying system, use the variation pattern defined by equation (61) with $\Delta f = 3$ N and $\tau = 4$ s. The block row number M was chosen to be 10. To show the capability of the algorithm to follow the system variation, the pseudodamped natural frequencies estimated using the noise-free responses are shown in Figures 9 (a) and (b). The results using three different values of N are compared with the true values. As expected, results show that the tracking ability of the algorithm is limited by N.

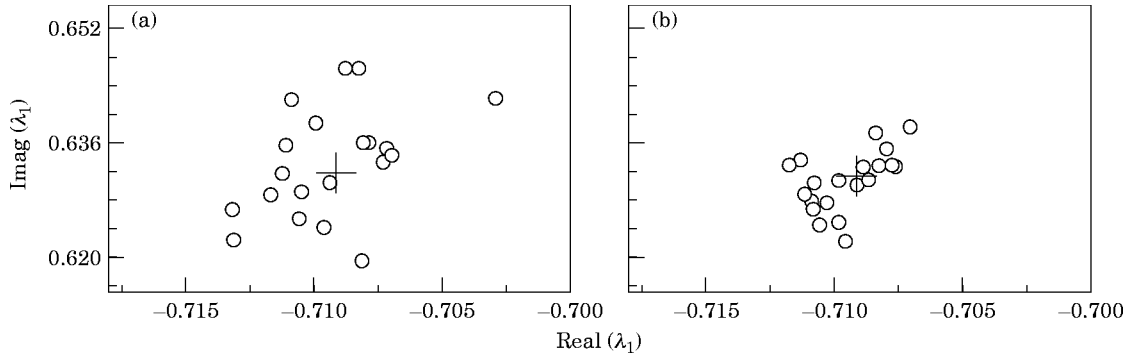

Figure 7. The estimated first eigenvalues of $\tilde{\mathbf{G}}(50, 0)$. (a) +, true; ○, estimate when $N = 6$; (b) +, true; ○, estimate when $N = 12$.

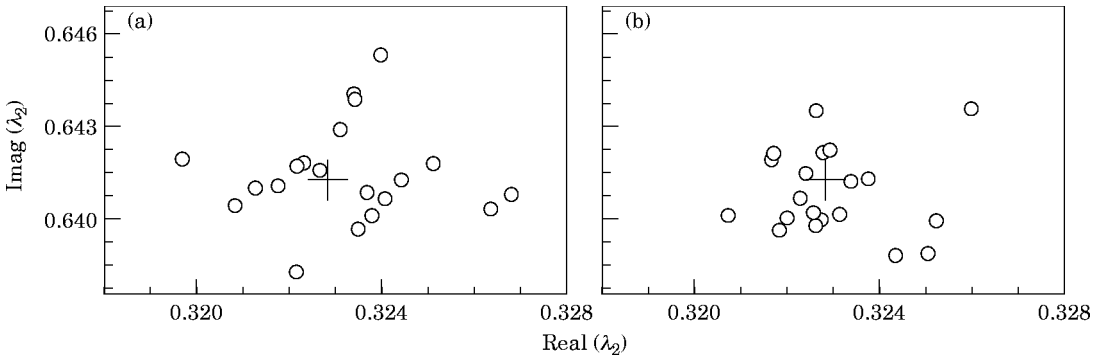

Figure 8. The estimated second eigenvalue of $\tilde{\mathbf{G}}(50, 0)$. (a) +, true; ○, estimate when $N = 6$; (b) +, true; ○, estimate when $N = 12$.

6. CONCLUSIONS

The identification of linear time-varying and freely vibrating systems has been addressed. A typical subspace-based technique for the model realization of linear time-invariant systems has been introduced. For time-varying systems, the development of the identification algorithm focuses on obtaining the varying transition matrix that shares the same eigenvalues as the original transition matrix. A key step of the proposed algorithm is to form a series of the general Hankel matrices using an ensemble of response sequences. Then the singular value decomposition is used to extract observability range spaces. The shift invariance structure preserved in two successive extracted subspaces is utilized to estimate the varying transition matrix at a moment. An approximate operation is conducted to ensure the invariability of the eigenvalues of the estimated transition matrix. The proposed algorithm has been extended to two special cases that require only a single response sequence, that is, periodically varying systems and slowly varying systems. The use of the eigenvalues of the estimated transition matrices has been discussed. The pseudomodal parameters have been defined by analogy to time-invariant systems. The physical interpretation of the pseudomodal parameters has been presented. Finally, an example of a two-link robot subject to a varying end force has been used to illustrate the proposed algorithms. The simulation has shown that the estimated pseudodamped natural

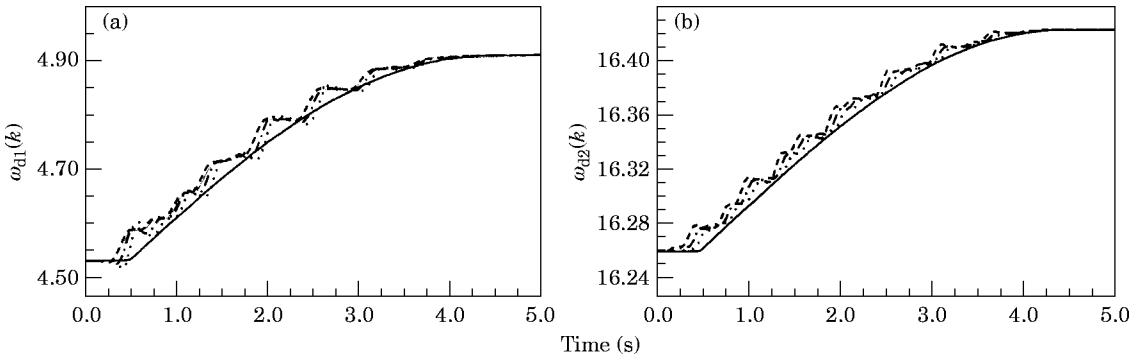

Figure 9. The estimated pseudodamped natural frequencies of the slowly varying system using the single noise-free response. (a) ——, true $\omega_{d1}(k)$; · · · · ·, estimated $\omega_{d1}(k)$ with $N=6$; ·–·–·–·, estimated $\omega_{d1}(k)$ with $N = 9$; - - - -, estimated $\omega_{d1}(k)$ with $N = 12$; (b) ——, true $\omega_{d2}(k)$; · · · · ·, estimated $\omega_{d2}(k)$ with $N=6$; ·–·–·–·, estimated $\omega_{d2}(k)$ with $N = 9$; - - - -, estimated $\omega_{d2}(k)$ with $N = 12$.

frequencies have a satisfactory tracking ability and the algorithm is adequately robust when the signal-to-noise is high or moderate.

REFERENCES

1. A. D. Sams 1985 *Ph.D. thesis*, *University of Southern California*, *Los Angeles*, *CA*. Identification of linear time-varying systems.
2. J. B. Allen and L. R. Rabiner 1977 *Proceedings of the IEEE* **65**, 1558–1564. A unified approach to short-time Fourier analysis and synthesis.
3. A. Benventiste 1987 *International Journal of Adaptive Control and Signal Processing* **1**, 3–39. Design of adaptive algorithms for the tracking of time-varying systems.
4. Y. Grenier 1983 *IEEE Transactions on Acoustics*, *Speech*, *and Signal Processing* **31**, 899–911. Time-dependent ARMA modeling of nonstationary signals.
5. M. Niedzwiecki 1990 *IEEE Transactions on Automatic Control* **35**, 610–616. Recursive functional series modeling estimators for identification of time-varying plants—more bad news than good?
6. J. B. McNeil, R. E. Kearney and I. W. Hunter 1992 *IEEE Transactions on Biomedical Engineering* **39**, 1213–1225. Identification of time-varying biological systems from ensemble data.
7. S. Shokoohi and L. Silverman 1987 *Automatica* **23**, 509–521. Identification and model reduction of time-varying discrete-time systems.
8. M. Verhaegen and X. Yu 1995 *Automatica* **31**, 201–216. A class of subspace model identification algorithms to identify periodically and arbitrarily time-varying systems.
9. C. S. Hsu and W. H. Cheng 1974 *Transactions of ASME*, *Journal of Applied Mechanics* **41E**, 371–378. Steady-state response of a dynamical system under combined parametric and forcing excitations.
10. G. L. Anderson 1985 *Journal of Sound and Vibration* **101**, 463–480. Stability of a manipulator with resilient joints.
11. A. M. Miyasar and A. D. S. Barr 1988 *Journal of Sound and Vibration* **124**, 79–89. The linear oscillator under parametric excitation with fluctuating frequency.
12. D. A. Streit, C. M. Krousgrill and A. K. Bajaj 1989 *Transactions of ASME*, *Journal of Dynamic System*, *Measurement*, *and Control* **111**, 470–480. Nonlinear response of flexible robotic manipulators performing repetitive tasks.
13. S. C. Sinha and G. J. Wiens 1989 *Journal of Sound and Vibration* **132**, 1–9. Response bounds for lumped vibrational systems with time-dependent parameters.
14. S. M. Shahruz and C. A. Tan 1989 *Journal of Sound and Vibration* **131**, 239–247. Response of linear slowly varying systems under external excitations.
15. K. Liu and M. R. Kujath 1994 *Journal of Sound and Vibration* **177**, 423–432. Response of slowly time-varying systems to harmonic excitation.
16. K. Liu 1992 *Ph.D. thesis*, *Technical University of Nova Scotia*, *Halifax*, *NS*. Vibrations of time-varying mechanical systems.
17. M. R. Kujath and K. Liu 1992 *Journal of Sound and Vibration* **156**, 481–504. On vibration of a class of linear time-varying systems.
18. A. D. Sams and V. Z. Marmarelis 1988 *Automatica* **24**, 563–567. Identification of linear periodically time-varying systems using white-noise test inputs.
19. M. Viberg 1995 *Automatica* **31**, 1835–1851. Subspace-based methods for the identification of linear time-invariant systems.
20. P. V. Overschee and B. D. Moor 1995 *Automatica* **31**, 1853–1864. A unifying theorem for three subspace system identification algorithms.
21. M. Deistler, K. Peternell and W. Scherrer 1995 *Automatica* **31**, 1865–1875. Consistency and relative efficiency of subspace methods.
22. J. N. Juang and R. S. Pappa 1985 *Journal of Guidance*, *Control and Dynamics* **8**, 620–627. An eigensystem realization algorithm for modal parameter identification and model reduction.
23. R. W. Longman and J. N. Juang 1989 *Journal of Guidance*, *Control and Dynamics* **12**, 646–652. Recursive form of the Eigensystem Realization Algorithm for system identification.
24. K. Liu and D. W. Miller 1995 *Transactions of ASME*, *Journal of Dynamic Systems*, *Measurement*, *and Control* **117**, 608–618. Time domain state space identification of structural systems.
25. A. M. King, U. B. Desai and R. E. Skelton 1988 *Automatica* **24**, 507–515. A generalized approach to q-Markov covariance equivalent realizations for discrete systems.

26. J. S. Lew, J. N. Juang and R. W. Longman 1993 *Journal of Sound and Vibration* **167**, 461–480. Comparison of several system identification methods for flexible structures.
27. K. Liu 1996 *Journal of Sound and Vibration* **197**, 387–402. Modal parameter estimation using the state space method.
28. G. H. Golub and C. F. Van Loan 1989 *Matrix Computations*. Baltimore, Maryland: The Johns Hopkins University Press.
29. M. Wax and T. Kailath 1985 *IEEE Transactions on Acoustics, Speech, and Signal Processing* **33**, 387–392. Detection of signals by information theoretic criteria.
30. H. D'Anglo 1970 *Linear Time-varying System: Analysis and Synthesis*. Boston: Allyn and Bacon.
31. L. A. Zadeh 1961 *Proceedings of the Institute Radio Engineers* **49**, 1488–1503. Time-varying networks, I.

APPENDIX A: MATRIX FORMULATIONS AND EVALUATION

A.1. AN APPROXIMATE FORMATION FOR $\mathbf{F}_1^+(k)\mathbf{F}_2(k+1)$ WHEN $n < p$

To find an approximate matrix for $\mathbf{F}_1^+(k)\mathbf{F}_2(k+1)$ when $n < p$, first determine the number of block rows using

$$n_r = \text{Ceil}(p/n), \tag{A1}$$

where Ceil$(\cdot)$ means to take the smallest whole number that is not less than p/n. Then let the first n_r block rows of $\mathbf{U}_p(k)$ be $\mathbf{F}_1(k)$ and the first n_r block rows of $\mathbf{U}_p(k+1)$ be $\mathbf{F}_2(k+1)$. For example, if $p = 4$ and $n = 2$, then $n_r = 2$ is used. In this case,

$$\mathbf{F}_1(k) = \begin{bmatrix} \mathbf{C}(k) \\ \mathbf{C}(k+1)\mathbf{G}(k+1,k) \end{bmatrix} \mathbf{T}^{-1}(k),$$

$$\mathbf{F}_2(k+1) = \begin{bmatrix} \mathbf{C}(k+1) \\ \mathbf{C}(k+2)\mathbf{G}(k+2,k+1) \end{bmatrix} \mathbf{T}^{-1}(k+1). \tag{A2}$$

Thus,

$$\mathbf{F}_1^+(k)\mathbf{F}_2(k+1) = \mathbf{T}(k)\mathbf{D}_1^{-1}\mathbf{D}_2\mathbf{T}^{-1}(k+1), \tag{A3}$$

where

$$\mathbf{D}_1 = \mathbf{C}^{\mathrm{T}}(k)\mathbf{C}(k) + \mathbf{G}^{\mathrm{T}}(k+1,k)\mathbf{C}^{\mathrm{T}}(k)\mathbf{C}(k)\mathbf{G}(k+1,k),$$

$$\mathbf{D}_2 = \mathbf{C}^{\mathrm{T}}(k+1)\mathbf{C}(k+1) + \mathbf{G}^{\mathrm{T}}(k+2,k+1)\mathbf{C}^{\mathrm{T}}(k+1)\mathbf{C}(k+1)\mathbf{G}(k+2,k+1). \tag{A4}$$

To ensure the existence of $\mathbf{F}_1^+(k)$, apparently $\mathbf{D}_1$ must be invertible.

A.2. NUMERICAL EVALUATION OF THE VARYING TRANSITION MATRICES

The varying transition matrices can be found using an ensemble of p states since $\mathbf{G}(k+1,k)$ satisfies a matrix equation given by

$$\mathbf{X}(k+1) = \mathbf{G}(k+1,k)\mathbf{X}(k), \tag{A5}$$

where

$$\mathbf{X}(k) = [\mathbf{x}_1(k) \quad \mathbf{x}_2(k), \ldots, \mathbf{x}_p(k)]$$

is the state matrix at moment k and

$$\mathbf{X}(k+1) = [\mathbf{x}_1(k+1) \quad \mathbf{x}_2(k+1), \ldots, \mathbf{x}_p(k+1)]$$

is the state matrix at moment $k + 1$. The true transition matrix can be found by

$$\mathbf{G}(k + 1, k) = \mathbf{X}(k + 1)\mathbf{X}^{-1}(k). \tag{A6}$$

To ensure the existence of $\mathbf{X}^{-1}(k)$, the p initial states must be independent of one another. In the example used in section 5, to evaluate the true transition matrices, four initial conditions formed a unit matrix, that is,

$$\mathbf{X}(0) = [\mathbf{x}_1(0) \quad \mathbf{x}_2(0) \quad \mathbf{x}_3(0) \quad \mathbf{x}_4(0)] = \mathbf{I}. \tag{A7}$$

The four state sequences were numerically found by the Runge–Kutta integrator.